

MICROSTRUCTURE AND INCLUSIONS OF IN-SITU AND ACID-RESIDUE PRESOLAR GRAPHITE GRAINS. P. Haenecour¹, J. Y. Howe^{1,2}, T. J. Zega^{1,3}, P. Wallace¹, S. Amari⁴, C. Floss⁴, K. Lodders⁵, K. Kaji⁶, T. Sunaoshi⁶ and M. Atsushi². ¹Lunar and Planetary Laboratory, University of Arizona, Tucson, AZ, USA. ²Hitachi High-Technologies America Inc., Clarksburg, USA. ³Dept. of Materials Science and Engineering, University of Arizona, Tucson, AZ, USA. ⁴Physics Department and Laboratory for Space Sciences, Washington University in St. Louis, St. Louis, MO, USA. ⁵Dept. of Earth and Planetary Sciences, Washington University in St. Louis, St. Louis, MO, USA. ⁶Hitachi High-Technologies Corporation, Ibaraki, Japan. (pierre@lpl.arizona.edu).

Introduction: Presolar graphite grains are known to condense in the envelopes of asymptotic giant branch stars and in the ejecta of stellar explosions [e.g., 1-5]. Previous transmission electron microscopy (TEM) studies of presolar graphite grains have shown that they exhibit various degrees of graphitization and commonly contain refractory inclusions (including carbides and metal grains) [e.g., 4, 5]. These studies have provided insights into the condensation conditions of presolar graphite grains and the environments in the stellar envelopes and ejecta in which they formed. Here we report on a comparison of the microstructures, elemental compositions, and inclusions of graphite grains identified *in-situ* in petrographic thin section and derived from acid-residue(s).

Samples and Experimental Methods. We prepared electron-transparent cross sections of five presolar graphite spherules, via previously described focused-ion-beam techniques [6], using the dual-beam Helios NanoLab 660 FIB-SEM at LPL: one grain (LAP-149) identified *in-situ* in a thin-section of the LaPaz Icefield (LAP) 031117 CO chondrite [7, 8] and four acid-residue grains from the Murchison CM chondrite [2] (Fig. 1). We then carried out energy-dispersive X-ray spectroscopy (EDS) and energy electron-loss spectroscopy (EELS) measurements of the grains using the newly developed Hitachi SU9000 30kV SEM/STEM located at LPL. The SU9000 is equipped with an Oxford Instruments X-Max 100LE EDS detector and Hitachi EELS system.

Results and Discussion: (1) Pre-accretionary Carbonaceous Rim On the Surface of Graphite Grain LAP-149. All presolar graphite grains studied so far with TEM were isolated and identified through a series of chemical dissolutions of samples of the Murchison or Orgeuil meteorites [2,3]. This process etched the surfaces of the grains, making it difficult to study the question: do presolar grains exhibit rims or coatings on their surfaces? However, analysis of grains identified *in situ* rectifies this problem, thus the presolar graphite grain (LAP-149) identified in a thin-section of LAP 031117 [6] allows us to investigate this question. The bright-field imaging reveals the presence of a small rim between the bottom of the graphite grain that was not exposed to the NanoSIMS Cs ion beam and the

surrounding matrix (Fig. 2). EDS mapping suggests that this rim appears to be composed of a mixture of carbonaceous material and silicate (elemental composition consistent with ferromagnesian silicate) (Fig. 2). EELS measurements (30 keV) show that the carbonaceous material is amorphous. Because grain LAP-149 was identified in a CO3.0 carbonaceous chondrite that experienced only minimal secondary processing (heating and aqueous alteration) [8], this rim might reflect ion bombardment in the CO nova ejecta, or interstellar or nebular processing of the grain surface before accretion of the meteorite parent body. Similar coatings of amorphous carbon were reported on the surfaces of presolar SiC grains gently isolated from the Murchison meteorite (“pristine presolar SiC” [9,10]). These authors suggested that the coatings could represent carbonaceous residues of processed ice mantles in the ISM and/or silica (SiO₂) rims due to oxidation of SiC grain surface in the solar nebula [9,10]. However, the rim surrounding graphite grain LAP-149 is clearly distinct from the surrounding matrix material and show a complex composition with both silicate and carbonaceous materials.

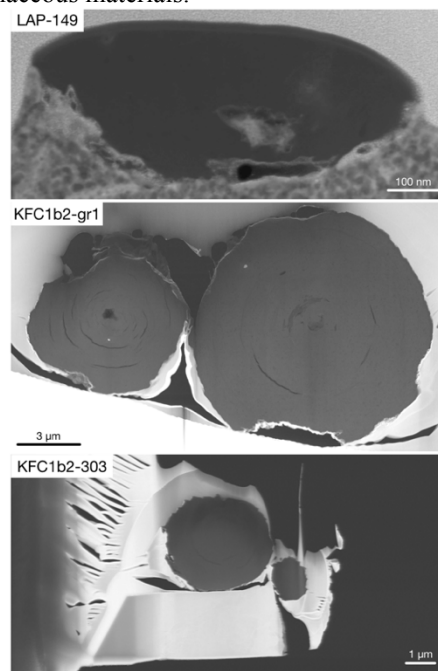


Fig 1. Dark-field (HAADF) STEM images of the five presolar graphite grains.

(2) Ferromagnesian Silicate-like Inclusion in Graphite LAP-149. Our STEM data also show the presence of a complex Si- and O-rich inclusion inside grain LAP-149. The EDS maps indicate heterogeneous distributions of Si and O across the inclusion, suggesting that it might be composed of several grains, including both silicate and oxide grains. While many different types of refractory inclusions have previously been reported inside of presolar SiC and graphite grains, to our knowledge, this is the first identification of a possible presolar silicate grain inside of a presolar graphite grain. The C, N and S isotopic composition of grain LAP-149 are all consistent with an origin in the ejecta a low-mass CO nova [6]. The identification of an O-rich inclusion inside of LAP-149 suggests the condensation of both C- and O-rich phases in the ejecta of low-mass CO nova. We will carry out equilibrium condensation calculations to model the condensation of this assemblage in a low-mass CO nova ejecta.

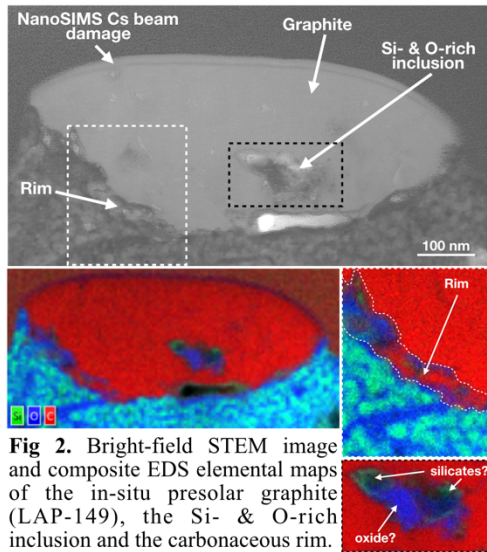


Fig 2. Bright-field STEM image and composite EDS elemental maps of the in-situ presolar graphite (LAP-149), the Si- & O-rich inclusion and the carbonaceous rim.

(3) Lithophile and Siderophile Elements in Inclusions Inside Presolar Graphites Grains. Isotopic studies of lithophile (e.g., Ba, Zr) and siderophile elements (e.g., Os and Mo) in unequilibrated chondrites using step leaching protocols have shown the survival of micrometer-scale isotopic anomalies [11-13]. These isotopic anomalies were interpreted as the products of *s*-process nucleosynthesis in stars before the solar system

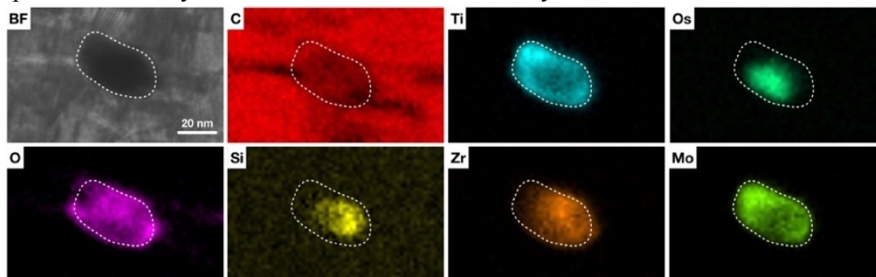


Fig. 3. Bright-field (BF) STEM image and false-color EDS elemental maps of an inclusion in graphite KFC1b2-gr1.

and carried by presolar carbonaceous grains (SiC and graphite grains) [11].

Bright-field STEM imaging and EDS mapping of refractory inclusions in two high-density graphite grains indicate that the graphite grain itself does not contain detectable amount of these lithophile and siderophile elements (e.g., Zr, Os, Mo) but that these elements are instead concentrated in inclusions inside the graphite grain (Fig. 3). One of the two inclusions appears to be composed of two distinct phases: a Si-rich phase containing significant amount of Zr and Os surrounded by a Ti- and Mo-rich oxide. This observation is consistent with previous TEM studies of inclusions in presolar graphites [14,15]. A previous CHARISMA analysis indicates that graphite grains most likely carry *s*-process anomalies [16].

Summary and ongoing work. Our new TEM data on the cross-section of presolar graphite grain LAP-149 shows that the grain's surface is coated with a mixture of silicate-like and C-rich material that likely reflects grain pre-accretionary surface processing in the nova ejecta, ISM or in the early solar nebula, before incorporation of the grain in the meteorite parent-body. Grain LAP-149 also contains a unique complex inclusion composed of both ferromagnesian silicate- and oxide-like material. Additional EDS analysis and electron diffraction of LAP-149 will help determine the detailed microstructures of the rim and silicate-like inclusion of grain LAP-149. We also identified two small refractory inclusions in the presolar graphite grain KFC1b2-gr1, that contain many trace elements (e.g., Os, Zr, Mo, Ru).

References. [1] Zinner (2014) in *Treatise on Geochemistry*, Vol 1.4, 181. [2] Amari et al. (2014) *GCA* 133, 479. [3] Jadhav et al. (2013) *GCA* 113, 193. [4] Croat et al. (2014) *Elements* 10, 441-446. [5] Gropman et al. (2012) *ApJL* 754 [6] Zega et al. (2007) *MAPS* 42, 1373. [7] Haenecour et al. (2016) *ApJ* 825. [8] Haenecour et al. (2017) *GCA* 221, 379. [9] Bernatowicz et al. (2003) *GCA* 67, 24, 4679. [10] Stroud et al. (2003). *LPSC XXXIV*, Abstract #1755. [11] Brandon et al. (2005) *Science* 309, 1233. [12] Dauphas et al. (2002) *ApJL* 569, L139. [13] Akram et al. (2015) *GCA* 165, 484. [14] Bernatowicz et al. (1996) *ApJ* 472, 760. [15] Croat et al. (2005) *ApJ* 631, 976. [16] Nicolussi et al. (1999) *ApJ* 504, 492.

Acknowledgments. This work is supported by NASA Grant NNX15AD94G for the NExSS “Earths in Other Solar Systems” (EOS) program. TEM and FIB analyses were carried out at the University of Arizona Kuiper Materials Imaging and Characterization Facility (NSF Grant 1531243 and NASA Grants NNX15AJ22G and NNX12AL47G).